

Reconstruction of Neumann eigenvalues and support of sound hard obstacles

Xiaodong Liu¹ and Jiguang Sun²

¹Institute of Applied Mathematics, Chinese Academy of Sciences.
Email: xdliu@amt.ac.cn

²Department of Mathematical Sciences, Michigan Technological University. Email: jiguangs@mtu.edu

Abstract

Recent study in inverse scattering theory shows that Dirichlet and transmission eigenvalues for sound soft obstacles and inhomogeneous non-absorbing media, respectively, can be reconstructed from scattering data. In this paper, we show that Neumann eigenvalues can be estimated from scattering data as well. It is done by choosing a point inside the obstacle and solving some linear ill-posed integral equations depending on the wavenumber. However, certain points inside the obstacle cannot be used for certain eigenvalues. Furthermore, we present some numerical study for the behavior of the solutions of the integral equations for points outside the obstacle. Finally, an eigenvalue method is employed to reconstruct the support.

1 Introduction

Recent study in inverse scattering theory shows that Dirichlet and transmission eigenvalues for sound soft obstacles and inhomogeneous non-absorbing media, respectively, can be reconstructed from scattering data [7, 8, 23] using qualitative methods such as the linear sampling method, the reciprocity gap method, the factorization method, etc., [11, 12, 13, 18, 19]. In this paper, we consider the problem of recovering Neumann eigenvalues for sound hard obstacles. Non-iterative methods using multiple frequency data in inverse scattering have been studied by only a few researchers. These methods include the multi-frequency obstacle reconstruction via the linear sampling method [15], the time domain linear sampling method [9], the time domain point source method [20], the enclosure method with dynamical data [16], the multi-frequency orthogonality sampling method [14], a multi-frequency linear sampling method using a frequency based partial variation approach [2], and the eigenvalue method [24].

We first study the reconstruction of Neumann eigenvalues for sound hard obstacles. We show that the Neumann eigenvalues can be estimated effectively from multiple frequency scattering data. In general, this is done by solving linear ill-posed integral equations at a point inside the obstacle and plotting the norm of the solutions as a function of the wavenumber. The value of the wavenumber

where a high spike appears is expected to be a Neumann eigenvalue. However, for certain points, some Neumann eigenvalues can not be recovered from the scattering data. This fact is taken into account when we use the eigenvalue method to reconstruct the sound hard obstacles. In addition, we perform some numerical study of the ill-posed integral equations for points outside the obstacle. To the best of the authors' knowledge, the paper contains the first numerical study of this kind.

The current paper completes the results in [7, 23, 24] in some sense. To be precise, corresponding to sound soft obstacles, sound hard obstacles, and inhomogeneous media, Dirichlet eigenvalues, Neumann eigenvalues, and transmission eigenvalues, respectively, can be computed from either far field or near field scattering data and be used to obtain the support of the scatterers.

The rest of the paper is organized as follows. In Section 2, we introduce the scattering problem by a sound hard obstacle and show that the Neumann eigenvalues can be estimated using multiple frequency scattering data by the linear sampling method. In Section 3, we employ the eigenvalue method to reconstruct sound hard obstacles using the eigenvalue indicator proposed in [24]. Finally, we draw some conclusions and discuss future works in Section 4.

2 The estimation of Neumann eigenvalues

Given the multiple frequency scattering data, we study the reconstruction of Neumann eigenvalues for sound hard obstacles using the linear sampling method. Let $D \subset \mathbb{R}^2$ be an open and bounded domain with Lipschitz boundary ∂D such that the exterior $D^e := \mathbb{R}^2 \setminus \overline{D}$ of \overline{D} is connected. Let k be the wavenumber and $S^1 := \{x \in \mathbb{R}^2 : |x| = 1\}$ denote the unit sphere in \mathbb{R}^2 . The fundamental solution of the Helmholtz equation in \mathbb{R}^2 is given by

$$\Phi(x, x_0, k) := \frac{i}{4} H_0^{(1)}(k|x - x_0|)$$

where $H_0^{(1)}$ denotes the Hankel function of the first kind of order zero. The two incident fields u^i of interest are plane waves $e^{ikx \cdot d}$, $d \in S^1$ and point sources $\Phi(x, x_0, k)$, $x_0 \in C$. The scattered field u^s is due to the scattering of the incident field u^i by D . For a sound hard obstacle, the scattered field u^s satisfies the following exterior boundary value problem with $f = -\partial u^i / \partial \nu$:

Given $f \in H^{-1/2}(\partial D)$ find $u^s \in H_{loc}^1(\mathbb{R}^2 \setminus \overline{D})$ such that

$$(2.1a) \quad \Delta u^s + k^2 u^s = 0 \quad \text{in } \mathbb{R}^2 \setminus \overline{D},$$

$$(2.1b) \quad \frac{\partial u^s}{\partial \nu} = f \quad \text{on } \partial D,$$

$$(2.1c) \quad \lim_{r \rightarrow \infty} \sqrt{r} \left(\frac{\partial u^s}{\partial r} - ik u^s \right) = 0,$$

where $r = |x|$ and ν is the unit outward normal to ∂D . The well-posedness of the above problem can be found in [12]. The corresponding eigenvalue problem is the Neumann eigenvalue problem.

It is shown in [12] that the scattered field u^s has the asymptotic behavior of

an outgoing spherical wave

$$(2.2) \quad u^s(x) = \frac{e^{ikr}}{\sqrt{r}} \left\{ u^\infty(\hat{x}) + O\left(\frac{1}{r}\right) \right\} \text{ as } r \rightarrow \infty,$$

uniformly in all directions $\hat{x} := x/r$ where the function $u^\infty(\hat{x})$ defined on S^1 is known as the far field pattern with \hat{x} denoting the observation direction.

2.1 Reconstruction by the linear sampling method

We denote the far field pattern of the scattered field for an incident plane wave given by $u^i(x, d) = e^{ikx \cdot d}$, $x \in \mathbb{R}^2$ with direction $d \in S^1$ by $u^\infty(\hat{x}, d)$, $\hat{x} \in S^1$. The scattered field for an incident point source $u^i(x, x_0) = \Phi(x, x_0, k)$ with source point $x_0 \in C$ is denoted by $u^s(x, x_0)$, $x \in \mathbb{R}^2 \setminus D$. The *inverse problem* we consider is to determine Neumann eigenvalues and reconstruct D from the knowledge of the far field $u^\infty(\hat{x}, d)$ or the near field data $u^s(x, x_0)$.

2.1.1 Far field observations

We assume that the far field patterns $u^\infty(\hat{x}, d)$ are given for all $\hat{x}, d \in S^1$. The far field operator $\mathcal{F} : L^2(S^1) \rightarrow L^2(S^1)$ is defined as

$$(2.3) \quad (\mathcal{F}g)(\hat{x}) = \int_{S^1} u^\infty(\hat{x}, d)g(d)ds(d), \quad \hat{x} \in S^1,$$

for $g \in L^2(S^1)$.

To reconstruct the target using the linear sampling method, one needs to solve the following linear ill-posed integral equations

$$(2.4) \quad (\mathcal{F}g)(\hat{x}) = \Phi^\infty(\hat{x}, z), \quad \hat{x} \in S^1,$$

for all $z \in T$ where T is a sampling domain inside Ω containing the target D . Here, $\Phi^\infty(\hat{x}, z) := e^{-ik\hat{x} \cdot z + i\pi/4} / \sqrt{8k\pi}$ is the far field pattern of the fundamental solution $\Phi(x, z)$. Next we define the Herglotz wave functions

$$v = \mathcal{H}g := \int_{S^1} e^{ikx \cdot d} g(d)ds(d), \quad g \in L^2(S^1).$$

The function g is called the Herglotz kernel of v . The function $\mathcal{F}g$ can be interpreted as the far field pattern which corresponds to the incident field $u^i = v$. We denote by $G : H^{-1/2}(\partial D) \rightarrow L^2(S^1)$ the operator mapping the boundary value $f \in H^{-1/2}(\partial D)$ to the far field pattern of the solution to (2.1a)-(2.1c). Hence $\mathcal{F} = -GH$ where $H : L^2(S^1) \rightarrow H^{-1/2}(\partial D)$ is an operator given by $Hg = \partial v / \partial \nu|_{\partial D}$, $g \in L^2(S^1)$.

In practice, one needs to deal with noisy data. Let \mathcal{F}^δ and G^δ be the operators corresponding to noisy measurement $u^{\infty, \delta}$ such that $\|G^\delta - G\| \leq \delta$. The linear sampling method usually seeks the Tikhonov regularization solutions of the linear ill-posed integral equations (2.4), i.e., the unique minimizer of the Tikhonov functional

$$(2.5) \quad \|\mathcal{F}^\delta g - \Phi^\infty(\cdot, z)\|_{L^2(S^1)}^2 + \epsilon \|g\|_{L^2(S^1)}^2$$

where ϵ is the regularization parameter. We denote $g_{z, \epsilon(\delta)}^\delta$ by $g_{z, \delta}$ when $\epsilon = \epsilon(\delta) \rightarrow 0$ as $\delta \rightarrow 0$. Then $1/\|g_{z, \delta}\|_{L^2(S^1)}$ is a characteristic function of the support of the scatterer D . We refer to [6, 18] for some theoretical analysis.

2.1.2 Near field observations

In the case of near field measurement, we assume that the scattered fields $u^s(\cdot, x_0)$ are available on $\Gamma = \partial\Omega$, a domain containing D , for all point sources x_0 on some closed curve C . The near field operator $\mathcal{N} : L^2(\Gamma) \rightarrow L^2(C)$ is defined as

$$(2.6) \quad (\mathcal{N}g)(x_0) = \int_{\Gamma} u^s(x, x_0)g(x)ds(x), \quad x_0 \in C,$$

for $g \in L^2(\Gamma)$. The near field counterpart of (2.4) is written as

$$(2.7) \quad (\mathcal{N}g)(x_0) = \Phi(x_0, z), \quad x_0 \in C.$$

Let $g_{z,\delta}$ be the the unique minimizer of the Tikhonov functional

$$(2.8) \quad \|\mathcal{N}^\delta g - \Phi(\cdot, z)\|_{L^2(C)}^2 + \epsilon \|g\|_{L^2(\Gamma)}^2.$$

Similar to the far field case, $1/\|g_{z,\delta}\|_{L^2(\Gamma)}$ is used to be a characteristic function of the support of the scatterer D .

2.2 Reconstruction of Neumann eigenvalues

Now we show how to reconstruct Neumann eigenvalues by the linear sampling method. It is shown in [7] that if k^2 is a Dirichlet or transmission eigenvalue, for almost every $z \in D$, the value $\|\mathcal{H}g_{z,\delta}\|_{H^1(D)}$ cannot be bounded as $\delta \rightarrow 0$, corresponding to the scattering of sound soft obstacles and inhomogeneous non-absorbing medium. We generalize the result in [7] to the case of the scattering by sound hard obstacles.

Theorem 2.1. *Assume that k^2 is a Neumann eigenvalue and the limit*

$$(2.9) \quad \lim_{\delta \rightarrow 0} \|\mathcal{F}^\delta g_{z,\delta} - \Phi^\infty(\cdot, z)\|_{L^2(S^1)} = 0,$$

holds for all $z \in D$. Then, for almost every $z \in D$, $\|\mathcal{H}g_{z,\delta}\|_{H^1(D)}$ cannot be bounded as $\delta \rightarrow 0$.

Proof. Assume on the contrary that $\|\mathcal{H}g_{z,\delta}\|_{H^1(D)} \leq M$ for some $M > 0$ and $z \in D_0 \subset D$ where D_0 has a positive measure. By the trace theorem there exists $c_1 > 0$ with $\|Hg_{z,\delta}\|_{H^{-1/2}(\partial D)} \leq c_1 \|\mathcal{H}g_{z,\delta}\|_{H^1(D)}$. Thus, combining the limit (2.9) and the inequality

$$\|\mathcal{F}^\delta g_{z,\delta} - \mathcal{F}g_{z,\delta}\| \leq \|G^\delta - G\| \|Hg_{z,\delta}\|_{H^{-1/2}(\partial D)},$$

we deduce that $\lim_{\delta \rightarrow 0} \|\mathcal{F}g_{z,\delta} - \Phi^\infty(\cdot, z)\|_{L^2(S^1)} = 0$. On the other hand, there exists a subsequence $v_n = \mathcal{H}g_{z,\delta_n}$ which converges weakly to some solution $v \in H^1(D)$ of Helmholtz equation $\Delta v + k^2 v = 0$ in D . Using again the trace theorem, $\|Hg_{z,\delta_n}\|_{H^{-1/2}(\partial D)}$ converges weakly to $\|\partial v / \partial \nu\|_{H^{-1/2}(\partial D)}$. By the compactness of the operator G , we conclude that

$$\|\mathcal{F}g_{z,\delta_n} - G(\partial v / \partial \nu|_{\partial D})\|_{L^2(S^1)} = \|GHg_{z,\delta_n} - G(\partial v / \partial \nu|_{\partial D})\|_{L^2(S^1)} \rightarrow 0$$

as $\delta \rightarrow 0$. Therefore $G(\partial v / \partial \nu|_{\partial D}) = \Phi^\infty(\cdot, z)$ on S^1 . Rellich's lemma and the unique continuation principle yield that $\partial v / \partial \nu = -\partial \Phi(\cdot, z) / \partial \nu$ on ∂D . Let

$w \in H^1(D)$ be a Neumann function corresponding to the eigenvalue k^2 . Then, with the help of the Green's theorem,

$$\begin{aligned} u(z) &:= \int_{\partial D} w(x) \frac{\partial \Phi(x, z)}{\partial \nu} ds(x) \\ &= \int_{\partial D} \left\{ v(x) \frac{\partial w(x)}{\partial \nu} - w(x) \frac{\partial v(x)}{\partial \nu} \right\} ds(x) \\ &= 0, \end{aligned}$$

for $z \in D_0$ and therefore for $z \in D$ by unique continuation. On the other hand u is a radiating solution in $\mathbb{R}^2 \setminus \overline{D}$ with homogeneous Neumann data $\partial v / \partial \nu = 0$ on ∂D . Here, we have used the continuity of the first derivative of the double-layer potential. Hence $u = 0$ in $\mathbb{R}^2 \setminus \overline{D}$. By the jump relation of the double-layer potential across ∂D we deduce that $w = 0$ on ∂D . Note that $\partial w / \partial \nu = 0$ on ∂D , using the Holmgren's uniqueness theorem we conclude that $w = 0$ in D . This contradicts the fact that w is a Neumann function and ends the proof. \square

Remark 2.2. *The limit (2.9) holds in many cases, e.g., if the operator \mathcal{F} has dense range. We refer to [7] for some examples when the limit (2.9) is valid independently from the scattering problem.*

Similar to the case of far field observations, if k^2 is a Neumann eigenvalue, we have the counterpart of Theorem 2.1 for the near field observations.

Theorem 2.3. *Assume that k^2 is a Neumann eigenvalue and the limit*

$$(2.10) \quad \lim_{\delta \rightarrow 0} \|\mathcal{N}^\delta g_{z, \delta} - \Phi(\cdot, z)\|_{L^2(C)} = 0,$$

holds for all $z \in D$. Then, for almost every $z \in D$, $\|\mathcal{S}g_{z, \delta}\|_{H^1(D)}$ cannot be bounded as $\delta \rightarrow 0$. Here,

$$(\mathcal{S}g)(x) = \int_{\Gamma} \Phi(x, y)g(y)ds(y), \quad x \in \mathbb{R}^2$$

is the single-layer potential with density g .

We hope that $\|\mathcal{S}g_{z, \delta}\|_{H^1(D)}$ plays the same role as $\|\mathcal{H}g_{z, \delta}\|_{H^1(D)}$ for the far field case. However, if k^2 is not a Neumann eigenvalue, the behavior of $\|\mathcal{S}g_{z, \delta}\|_{H^1(D)}$ is not known yet for the case of near field observations. Nevertheless, the numerical examples below give the expected results.

Let $g_{z, \delta}$ be the unique minimizer of the Tikhonov functional (2.5). In [3], Arens and Lechleiter proved that, if k^2 is not a Neumann eigenvalue and if $z \in D$, the Herglotz wave function $\mathcal{H}g_{z, \delta}$ with kernel $g_{z, \delta}$ converges in the $H^1(D)$ as $\delta \rightarrow 0$. Thus for $z \in D$, if we plot the norms of the Herglotz kernels of the regularized solutions against the wavenumber, we would expect the norms are relatively large when k^2 is a Neumann eigenvalue and relatively small otherwise. However, it would be desirable to obtain a clear picture of the behavior of the norms of Herglotz kernels as the wavenumber approaches a Neumann eigenvalue k_* .

For effective reconstruction of the Neumann eigenvalues, we would like to know how many wavenumbers are necessary in the unit interval. To start discussion, we need some results of the interior Neumann problem. Let

$$(u, v) = \int_D u \bar{v} dx, \quad \text{for all } u, v \in L^2(D).$$

and

$$V = \left\{ v \in H^1(D) : \int_D v(x) dx = 0 \right\}.$$

Then V is compactly imbedded in $L^2(D)$ (see [1] or Theorem 3.6 of [21]). In addition, we assume that D is a bounded domain that can be written as a finite union of domains that are star-shaped with respect to a ball. It is known that

$$a(u, v) = (\nabla u, \nabla v)$$

is coercive on V (see Section 4.2 of [4]). Assuming k^2 is not a Neumann eigenvalue, we consider the interior Neumann boundary value problem to find $v_z \in V$ such that

$$(2.11a) \quad \Delta v_z + k^2 v_z = 0, \quad \text{in } D,$$

$$(2.11b) \quad \frac{\partial v_z}{\partial \nu} + \frac{\partial \Phi(\cdot, z, k)}{\partial \nu} = 0, \quad \text{on } \partial D.$$

The corresponding Neumann eigenvalue problem is to find $(\lambda, u) \in \mathbb{R} \times V$ such that

$$(2.12a) \quad (\nabla u, \nabla \phi) = \lambda(u, \phi), \quad \text{for all } \phi \in V,$$

$$(2.12b) \quad \frac{\partial u}{\partial \nu} = 0, \quad \text{on } \partial D.$$

Let $\theta := \Phi(\cdot, z, k)\chi$ where χ is a C^∞ cutoff function which is one in a neighborhood on ∂D and zero in a neighborhood of z . Furthermore, we choose χ is such that $\partial \theta / \partial \nu = \partial \Phi / \partial \nu$ on ∂D as well.

Let $A : V \rightarrow V$ and $B : V \rightarrow V$ be given by

$$(A\varphi, \psi)_{H^1(D)} = (\nabla \phi, \nabla \psi) \quad \text{and} \quad (B\psi, \phi)_{H^1(D)} = (\phi, \psi),$$

respectively. We also define a functional $l_{z,k}$ on V

$$(2.13) \quad (l_{z,k}, \psi)_{H^1(D)} = (\nabla \theta, \nabla \phi) - k^2(\theta, \phi), \quad \text{for all } \psi \in V.$$

Letting $\varphi := v_z - \theta$ one has that

$$\begin{aligned} (\Delta \varphi + k^2 \varphi, \phi) &= (\Delta v_z, \phi) + k^2(v_z, \phi) - (\Delta \theta, \phi) + k^2(\theta, \phi) \\ &= -(\nabla v_z, \nabla \phi) + k^2(v_z, \phi) + \int_{\partial D} \frac{\partial v_z}{\partial \nu} \phi ds \\ &\quad + (\nabla \theta, \nabla \phi) - k^2(\theta, \phi) - \int_{\partial D} \frac{\partial \theta}{\partial \nu} \phi ds \\ &= (l_{z,k}, \phi). \end{aligned}$$

Then the Neumann boundary value problem for φ can be written as

$$(2.14) \quad A\varphi - k^2 B\varphi = -l_{z,k}.$$

It is clear that A is a bounded self-adjoint positive definite operator which has a bounded inverse. In addition, $B : V \rightarrow V$ is compact. To see this, let

$\{u_j\}$ be a bounded sequence in V . Due to the compact imbedding of $H^1(D)$ into $L^2(D)$, there is a convergent subsequence $\{u_{j_k}\}$ of $\{u_j\}$ in $L^2(D)$.

$$\begin{aligned}\|Bu\|_{H^1(D)}^2 &= (Bu, Bu)_{H^1(D)} = (u, Bu)_{L^2(D)} \\ &\leq \|u\|_{L^2(D)}\|Bu\|_{L^2(D)} \leq \|u\|_{L^2(D)}\|Bu\|_{H^1(D)}.\end{aligned}$$

Thus $\|Bu\|_{H^1(D)} \leq \|u\|_{L^2(D)}$ and $\{Bu_{j_k}\}$ is a Cauchy sequence in V since $\{u_{j_k}\}$ is a Cauchy sequence. Hence $\{Bu_{j_k}\}$ converges in V .

For the behavior of the kernel of the approximate solution for the far-field equation, we have the following theorem.

Theorem 2.4. *Let k_*^2 be a Neumann eigenvalue for $-\Delta$ in D and $\alpha > 0$ such that the ball*

$$B_{k_*^2, \alpha} := \{k^2 : |k^2 - k_*^2| < \alpha, k^2 \neq k_*^2\}$$

does not contain any Neumann eigenvalues other than k_^2 . Let g_z^ϵ be an approximate solution of the far-field equation. Then for sufficient small $\epsilon > 0$ and $\alpha > 0$, and almost every $z > 0$ one has that*

$$\|v_{g_z^\epsilon}\|_{H^1(D)} \geq \frac{C_1}{|k^2 - k_*^2|} \quad \text{and} \quad \|g_z^\epsilon\|_{L^2(\Omega)} \geq C_2|k^2 - k_*^2|$$

for all $k^2 \in B_{k_^2, \alpha}$ where v_g is the Herglotz wave function and C_1 and C_2 are the positive constants dependent on z , k_* and α , but not on k and ϵ .*

The proof is similar to that of Theorem 5 in [15] with suitable changes of the functional spaces for sound-hard obstacles. We give it here only for completeness.

Proof. Let T be the compact self-adjoint operator given by $T := A^{-1/2}BA^{-1/2} : V \rightarrow V$. If k_*^2 is a Neumann eigenvalue, $\lambda_* = 1/k_*^2$ is an eigenvalue of T . Let E and M be the eigenspaces and generalized eigenspaces for T , respectively. The resolvent $R(\xi) = (T - \xi)^{-1}$ has a Laurent series expansion in a neighborhood of λ_* [17]

$$R(\xi) = -\frac{P}{\xi - \lambda_*} - \sum_{p=1}^{\infty} \frac{Q^p}{(\xi - \lambda_*)^{p+1}} + \sum_{p=0}^{\infty} (\xi - \lambda_*)^p S^{p+1}.$$

Here p is the least integer such that $(T - \lambda_* I)^p w = 0$ for all $w \in M$,

$P : V \rightarrow M$ is the orthogonal projection,

$Q = (T - \lambda_* I)P$ is the eigen-nilpotent projection such that $Q = PQ = QP$,

and S is a bounded operator satisfying $(T - \lambda_* I)S = I - P$ such that $SP = PS = 0$.

It is easy to see that $Q^j = 0$ if $j \geq m := \dim M$ and the range of Q^{m-1} is a subset of E .

If k^2 is not a Neumann eigenvalue for D , then

$$k^2(T - \xi I)A^{1/2}\varphi = A^{-1/2}l_{z,k}$$

and thus

$$k^2 A^{1/2}\varphi = R(\xi)A^{-1/2}l_{z,k}$$

where $\varphi = v_z - \theta$. Using the expansion for $R(\xi)$, one has that

$$k^2 A^{1/2} \varphi = -\frac{PA^{-1/2}l_{z,k}}{\xi - \lambda_*} - \sum_{p=1}^{m-1} \frac{Q^p A^{-1/2}l_{z,k}}{(\xi - \lambda_*)^{p+1}} + \sum_{p=0}^{\infty} (\xi - \lambda_*)^p S^{p+1} A^{-1/2}l_{z,k}.$$

Thus

$$\begin{aligned} \|k^2 A^{1/2} \varphi\| &= \frac{1}{(\xi - \lambda_*)^m} \left\| Q^{m-1} A^{-1/2}l_{z,k} + \sum_{p=1}^{m-2} (\xi - \lambda_*)^{m-p-1} Q^p A^{-1/2}l_{z,k} \right. \\ &\quad \left. + (\xi - \lambda_*)^{m-1} P A^{-1/2}l_{z,k} - \sum_{p=0}^{\infty} (\xi - \lambda_*)^{p+m} S^{p+1} A^{-1/2}l_{z,k} \right\|. \end{aligned}$$

Substituting $\xi = 1/k^2$ and $\lambda = 1/k_*^2$, due to the fact that A, Q, S are bounded operators and $l_{z,k}$ is uniformly bounded for α small enough, one has that

$$\|k^2 A^{1/2} \varphi\| \geq \frac{|k^2 k_*^2|^m}{|k^2 - k_*^2|^m} \|Q^{m-1} A^{-1/2}l_{z,k}\|_{H^1(D)} - C_p,$$

where $C_p \geq 0$ depends on z and k_* , but not on k .

Now it is suffice to show that $Q^{m-1} A^{-1/2}l_{z,k} \neq 0$ for almost all $z \in D$. If this is true, then

$$\|Q^{m-1} A^{-1/2}l_{z,k}\| \geq \frac{1}{2} \|Q^{m-1} A^{-1/2}l_{z,k_*}\|$$

for $k^1 \in B_{k_*^2, \alpha}$ and sufficiently small $\alpha > 0$ due to continuity. Then one would have that

$$\|k^2 A^{1/2} \varphi\|_{H^1(D)} \geq \frac{|k^2 k_*^2|^m}{2|k^2 - k_*^2|^m} \|Q^{m-1} A^{-1/2}l_{z,k_*}\|_{H^1(D)} - C_p, \quad m \geq 1.$$

Obviously, $C_p \approx O(1)$ as $\alpha \rightarrow 0$ which implies

$$\|A^{1/2} \varphi\|_{H^1(D)} \geq \frac{C}{|k^2 - k_*^2|} \|Q^{m-1} A^{-1/2}l_{z,k_*}\|_{H^1(D)}, \quad k^2 \in B_{k_*^2, \alpha}$$

where C is a positive constant independent of k such that $0 < C < \frac{1}{2}|k^2 k_*^2|^m$. Since $A^{-1/2}$ and Q are bounded operators, l_{z,k_*} is bounded, χ vanishes in a neighborhood of z , and $Q^{m-1} A^{-1/2}l_{z,k_*} \neq 0, q \geq 0$ for almost $z \in D$, the above inequality implies

$$\|v_z\|_{H^1(D)} \geq \left| \|\varphi\|_{H^1(D)} - \|\Phi(\cdot, z, k)\chi(\cdot)\|_{H^1(D)} \right| \geq \frac{C'}{|k^2 - k_*^2|} - C'' \geq \frac{C'''}{|k^2 - k_*^2|}$$

for suitably chosen constant $C''' > 0$ dependent on z, k_* and α , but not on k .

In the rest of the proof, we show that $Q^{m-1} A^{-1/2}l_{z,k} \neq 0$ for almost all $z \in D$. Assume that

$$Q^{m-1} A^{-1/2}l_{z,k_*} = 0.$$

Thus $A^{-1/2}l_{z,k_*}$ is orthogonal to at least one eigenvector, say u_* in E . To see this, note that T is a compact self-adjoint operator on the Hilbert space V , thus $M = E$ (see Page 683 in [5]). If $m = 1$, then $A^{-1/2}l_{z,k_*} = 0$ and the result is

Table 1: Square roots of Neumann eigenvalues of different obstacles.

Domain	1st	2nd	3rd
circle	3.6874	6.1246	7.6987
unit square	π	$\sqrt{2}\pi$	2π
triangle	4.1891	7.2367	8.3800
ellipse	3.1072	4.5070	5.5974

trivial. Let $V = E \oplus E^\perp$ and $A^{-1/2}l_{z,k_*} = x + y$ for $x \in E$ and $y \in E^\perp$. If $\dim E = m > 1$, it is obvious that we can find a $u_* \in E$ such that $(x, u_*) = 0$. Since $(y, u_*) = 0$, we obtain $(A^{-1/2}l_{z,k_*}, u_*) = 0$.

Since $A^{-1/2}$ is self-adjoint, one has that $(l_{z,k_*}, A^{-1/2}u_*) = 0$. Noting that $(I - k_*^2 A^{-1/2} B A^{-1/2})u_* = 0$, one obtains

$$A^{-1/2}(A - k_*^2 B)A^{-1/2}u_* = 0.$$

This requires that l_{z,k_*} be orthogonal to an element in the kernel of $(A - k_*^2 B)$. Thus l_{z,k_*} is orthogonal to an eigenfunction corresponding to Neumann eigenvalue k_*^2 . Let ϕ_* denote this Neumann eigenfunction. By the first Green's identity, one has that

$$0 = (l_{z,k_*}, \phi_*)_{H^1(D)} = \int_D \nabla \theta \cdot \nabla \bar{\phi}_* - k_*^2 \theta \bar{\phi}_* dx = \int_{\partial D} \frac{\partial \bar{\phi}_*}{\partial \nu} \Phi(x, z, k_*) ds_x,$$

for $z \in D$. We define

$$w(z) := \int_{\partial D} \frac{\partial \bar{\phi}_*}{\partial \nu} \Phi(z, x, k_*) ds_x$$

due to the symmetry of Φ . Hence $w(z) = 0$ for all $z \in \mathcal{Z} \subset D$. Then $w(z) = 0$ in D due to the unique continuity. By the continuity of the single layer potential, $w(z) = 0$ on ∂D . This implies that $w(z) = 0$ in $\mathbb{R}^2 \setminus \bar{D}$ since w is a radiating solution to the exterior Dirichlet problem with zero boundary data. Thus $\frac{\partial \bar{\phi}_*}{\partial \nu} = 0$ on ∂D which contradicts the assumption that ϕ_* is a Neumann eigenfunction and the proof is complete. \square

In the following, we show some numerical examples. We use the four objects as above and assume that the support of D is known (approximately) a priori which can be obtained using the linear sampling method, etc. [6, 11, 13, 22, 18]. We choose an appropriate interval for each obstacle and partition the interval. For each wavenumber k in the partition, we record the scattered field u^s on Γ and add 3% normally distributed noise. Then we choose a point z inside the obstacle D and solve the ill-posed integral equation (2.7) using Tikhonov regularization with Morozov discrepancy [12]. Finally we plot the norm of the Herglotz kernel g against the wavenumber k . The square roots of Neumann eigenvalues should be the locations where a spike can be spotted.

We choose an interval $F = [2, 8]$ and partition it using $N = 301$ in view of Theorem 2.4:

$$(2.15) \quad F_k = \left\{ 2 + i \times \frac{8-2}{N-1}, i = 0, 1, 2, \dots, N-1 \right\}.$$

We compute the Tikhonov regularized solution and plot the norm of the Herglotz kernel v.s. the wavenumber in Fig. 1 for $z = (0.2, 0.1)$ inside the targets. It can be seen that the pictures have clear spikes indicating the locations of Neumann eigenvalues.

For verification, we also compute a few lowest Neumann eigenvalues using a finite element method and show them in Table 1. The dotted vertical lines in Fig. 1 are the exact Neumann eigenvalues. Comparing with the values in Table 1, we see that the spikes in Fig. 1 and the Neumann eigenvalues in Table 1 coincide very well.

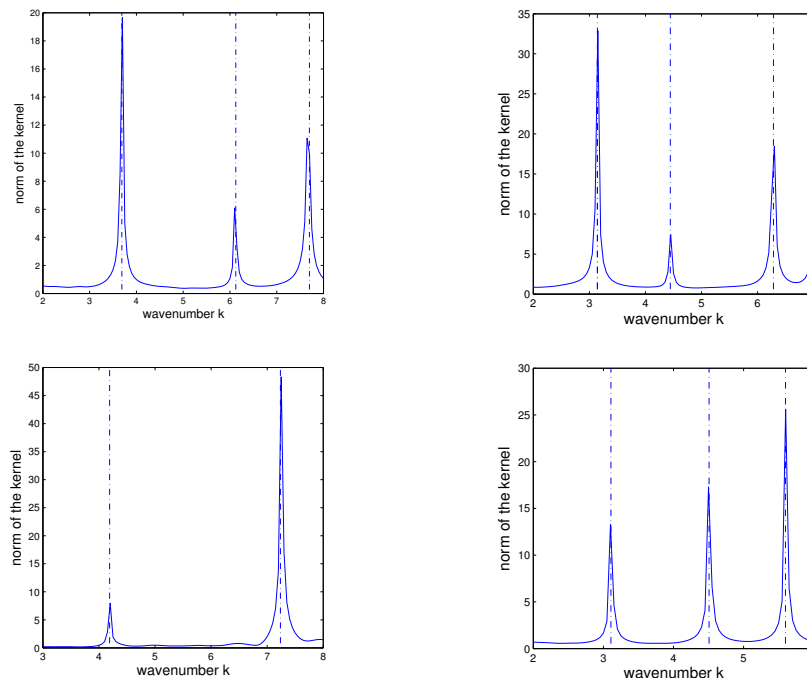


Figure 1: Reconstruction of the Neumann eigenvalues (the norm of the Herglotz kernel of the regularized solutions for $z = (0.2, 0.1)$ inside the target v.s. the wavenumber). The dotted lines are locations of the square roots of the exact Neumann eigenvalues. Top left: A disk with $r = 1/2$. Top Right: The unit square. Bottom left: A triangle. Bottom right: An ellipse with $a = 0.6, b = 0.4$.

To test the robustness of the reconstruction, we show the reconstruction using different amount of noise in Fig. 2. With 10% of noise, the reconstruction start to have some spikes formed at locations other than Neumann eigenvalues. However, it seems that the first Neumann eigenvalue can be identified even with 20% of noise.

Theorems 2.1 and 2.3 hold for almost every $z \in D$. However, for certain points, $\|\mathcal{H}g_{z,\delta}\|_{H^1(D)}$ may not be unbounded for certain Neumann eigenvalue k , i.e., a spike will not be formed at some eigenvalue k . Fig. 3 shows similar plots as in Fig. 1 but with a different point $z = (0, 0)$. If we compare two figures, we can see that, for $z = (0, 0)$, the lowest two Neumann eigenvalues of the circle

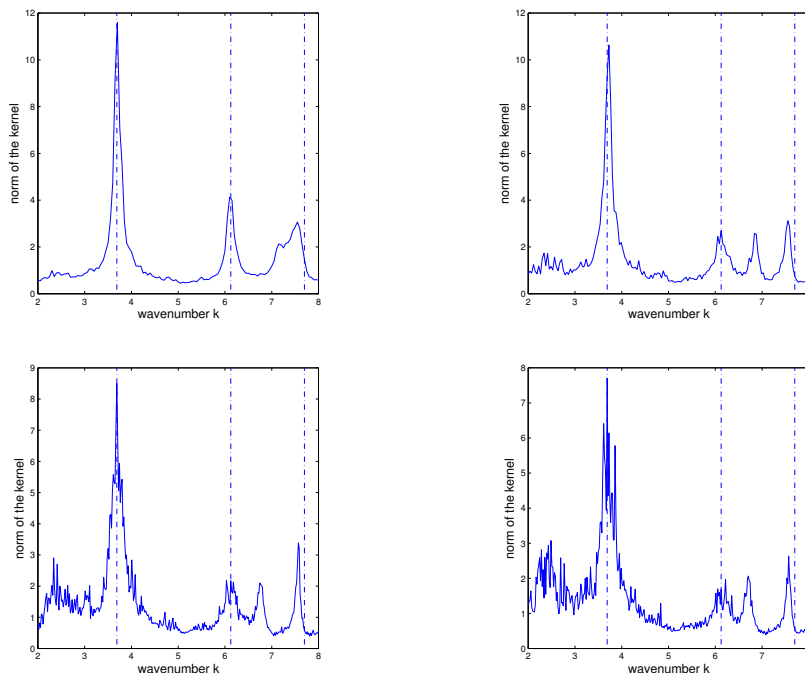


Figure 2: Reconstruction of the Neumann eigenvalues (the norm of the Herglotz kernel of the regularized solutions for $z = (0.2, 0.1)$ inside the target v.s. the wavenumber) for the disc with $r = 1/2$. The dotted lines are locations of the square roots of the exact Neumann eigenvalues. Top Left: with 5% normally distributed noise. Top Right: with 10% normally distributed noise. Bottom Left: with 15% normally distributed noise. Bottom Right: with 20% normally distributed noise.

are missed, the lowest two Neumann eigenvalues of the unit square are missed, the lowest Neumann eigenvalue of the triangle is missed, and the lowest two Neumann eigenvalues of the ellipse are missed. One way to fix this is to use multiple random points inside the obstacle and combine the result. We refer the reader to [8] for details.

The following theorem points out that, for points z outside of \bar{D} , $\|\mathcal{H}g_{z,\delta}\|_{H^1(D)}$ is always unbounded as $\delta \rightarrow 0$ if the limit (2.9) holds.

Theorem 2.5. *For every $z \notin D$, assume that (2.9) (or (2.10) in the case of near field observations) holds. Then $\|\mathcal{H}g_{z,\delta}\|_{H^1(D)}$ (or $\|\mathcal{S}g_{z,\delta}\|_{H^1(D)}$ in the case of near field observations) is always unbounded as $\delta \rightarrow 0$.*

Proof. We only prove the case of far field observations, the near field case can be dealt with similarly.

Assume on the contrary that $\|\mathcal{H}g_{z,\delta_n}\|_{H^1(D)} \leq M$ for some $M > 0$ and some sequence $\delta_n \rightarrow 0$. Then there exists a subsequence of $v_n = \mathcal{H}g_{z,\delta_n}$ which converges weakly to some $v \in H^1(D)$. Let v^s be the radiating solution of the Helmholtz equation in $\mathbb{R}^2 \setminus \bar{D}$ with Neumann boundary data $\partial v / \partial \nu$ on ∂D and

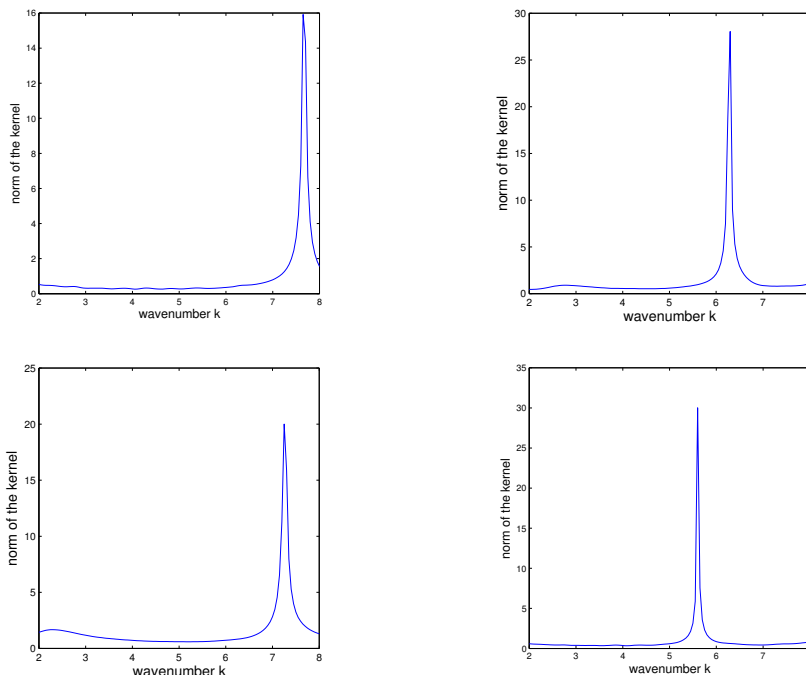


Figure 3: We show that it is not possible to estimate some Neumann eigenvalues if we choose certain points. The point is chosen to be $z = (0, 0)$ for all examples. Top Left: the circle. Top Right: the unit square. Bottom Left: the triangle. Bottom Right: the ellipse.

v^∞ be the corresponding far field pattern. From the arguments in the proof of Theorem 2.1, we know that $\lim_{\delta \rightarrow 0} \|Fg_{z, \delta_n} - \phi_z\|_{L^2(S^1)} = 0$. Since Fg_{z, δ_n} is the far field pattern of the scattered field with Neumann boundary data $-\partial v_n / \partial \nu$ on ∂D we conclude that $Fg_{z, \delta_n} \rightarrow v^\infty$ and thus $v^\infty = \phi_z$. Rellich's lemma and unique continuation principle imply $v^s = \Phi(\cdot, z)$ in $\mathbb{R}^2 \setminus (D \cup \{z\})$. This leads to a contradiction since $v^s \in H_{loc}^1(\mathbb{R}^2 \setminus \overline{D})$ while this is not the case for $\Phi(\cdot, z)$. The proof is complete. \square

Remark 2.6. *The above is true for the Dirichlet and Transmission eigenvalues as well.*

In general, when $z \in \mathbb{R} \setminus \overline{D}$, the solution of the ill-posed integral equation is unbounded for all wavenumbers. In Fig. 4, we show the plots of the norm of the kernels when z is chosen to be outside D . It can be seen that although at some eigenvalues, spikes can be formed. But they are far from the clear plots in Fig. 1. Moreover, when the wavenumber is not a Neumann eigenvalue, the norm of the solution is not bounded as predicted by the linear sampling method [6].

In the following, we check how the plots change when we move z from inside to outside of the scatterer. We choose the circle and show the plot of the norm of the kernel of the solutions in Fig. 5. For $z = (0.5, 0.5)$, which is outside the

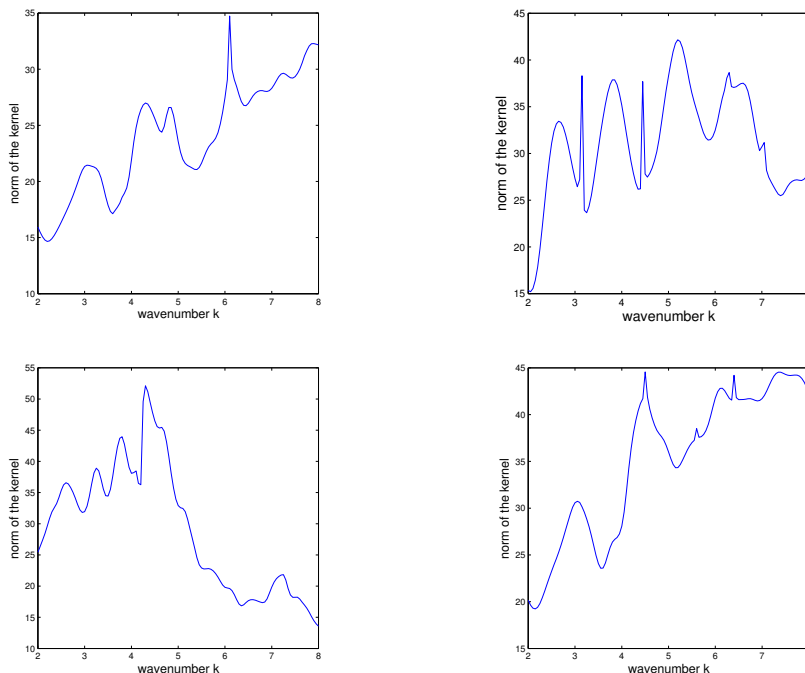


Figure 4: The plots of the norms of the Herglotz kernels v.s. the wavenumber when $z = (0.7, 0.7)$ which is outside the scatterers. Top Left: the circle. Top Right: the unit square. Bottom Left: the triangle. Bottom Right: the ellipse.

obstacle, we still see the spikes. However, the third spike is missing in contrast with the plot for $z = (0.3, 0.3)$. In addition, in the top right plot, the first two spikes are not reconstructed as good as the top left plot.

3 Reconstruction of sound hard obstacles

In this section, we employ the eigenvalue method proposed in [24] to reconstruct the sound hard obstacles. We do not assume any a priori information of the target unless a domain which contains the target, i.e., we do not assume that we know a point in D as in the previous section.

Let Λ be the set of Neumann eigenvalues. We assume that an interval $F = [a, b]$ is chosen such that $\Lambda \cap F \neq \emptyset$ and consider a partition $F_k = \{k_i, i = 0, \dots, N\}$ of F . For simplicity, we assume that the lowest Neumann eigenvalue is in F . Note that the condition $\Lambda \cap F \neq \emptyset$ is not a restrictive requirement since one can choose a small enough and b large enough.

Let $v(y, k_i)$ be the Herglotz wave function. The multiple frequency near field integral operator is defined as

$$(3.16) \quad (\mathcal{N}v)(x, k_i) = \int_{\Gamma} u^s(y, x, k_i)v(y, k_i)ds(y), \quad x \in C, \quad k_i \in F_k.$$

For each point $z \in T$, a sampling domain containing D , the near field integral

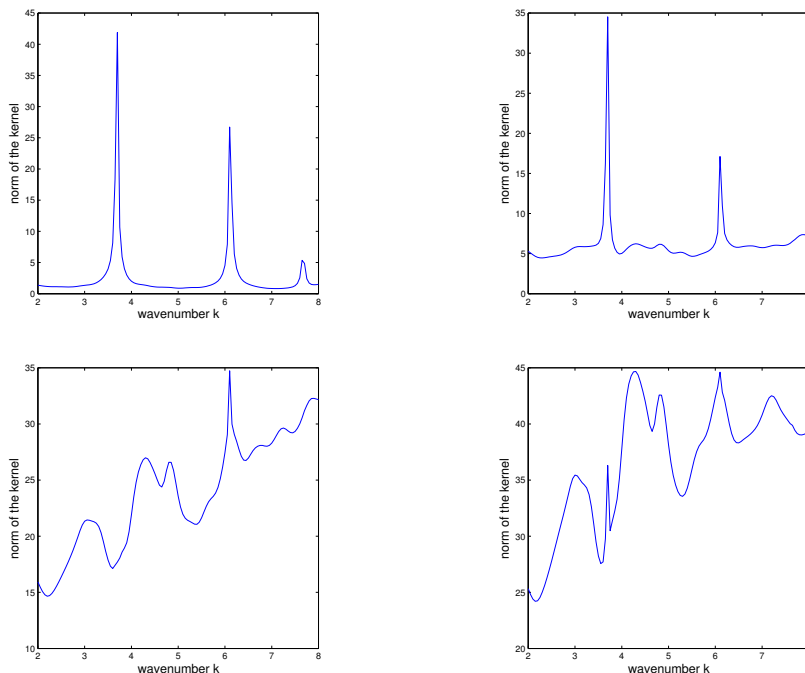


Figure 5: The plots of the norm of the Herglotz kernel against the wavenumber with z 's from inside to outside the circle. Top Left: $z = (0.3, 0.3)$. Top Right: $z = (0.5, 0.5)$ Bottom Left: $z = (0.7, 0.7)$. Bottom Right: $z = (0.9, 0.9)$.

equation is defined as

$$(3.17) \quad (\mathcal{N}v)(\cdot, k_i) = \Phi(\cdot, z, k_i), \quad k_i \in F_k.$$

For each $z \in T$ and wavenumber k_i in F_k , we compute the regularized solutions and denote the norm of the Herglotz kernel of the regularized solution for (3.17) by $H_z(k_i)$. The eigenvalue indicator is defined as

$$(3.18) \quad I_z = \frac{\max_i H_z(k_i)}{\sum_i H_z(k_i)/N_k}, \quad z \in T.$$

If $z \in D$, we expect to find a spike corresponding to a Neumann eigenvalue which implies a large value of I_z . For z outside the obstacles, we have seen in Fig. 4 that no obvious spikes indicating that the value of I_z is relatively small.

Now we show some numerical examples for sound hard obstacles. We choose a sampling domain T given by $[-1, 1] \times [-1, 1]$ containing D . For the disk with radius $r = 1/2$, we set $F = [3.2, 4.2]$ and

$$(3.19) \quad F_k = \left\{ 3.2 + i \times \frac{4.2 - 3.2}{20}, i = 0, 1, 2, \dots, 20. \right\}.$$

Similarly, we choose $F = [2.6, 3.6]$, $F = [3.6, 4.6]$, and $F = [2.6, 3.6]$ for the unit square, the triangle, and the ellipse, respectively. From Table 1, we know that

all these intervals contain Neumann eigenvalues for the circle, the square, the triangle, and the ellipse, respectively. We solve the near field equations for each k_i at the sampling point z and compute the indicator functions defined in (3.18) for all sampling points.

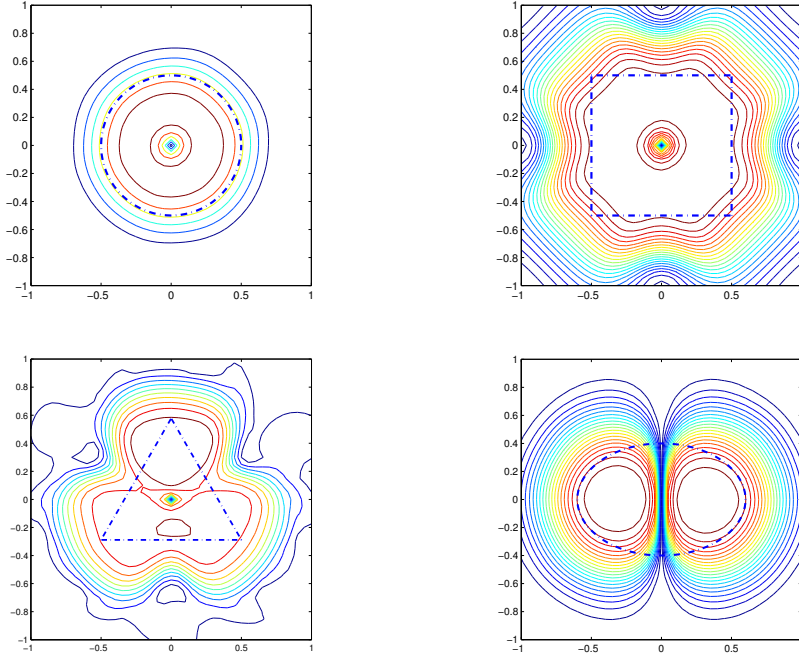


Figure 6: Reconstruction of the sound hard obstacles using the eigenvalue indicator.

In Fig. 6, we show the plots of the indicator function I_z . The dotted lines are the exact boundaries. We can see that the values of the indicator functions are small for $z = (0, 0)$, centers of the circle, the unit square, and the triangle. For the ellipse, the values are small for all points on the y-axis. This is related to the inability to reconstruct certain Neumann eigenvalues we saw in the previous section. To correct this, we choose a larger interval $[2, 8]$ which contains multiple eigenvalues. We expect that at least one eigenvalue is reconstructed for each z in the sampling domain. In Fig. 7 we show the result of the eigenvalue method using a reasonable larger intervals for the wave numbers.

As the linear sampling method, we need to choose a contour as the reconstruction of the obstacles. Since the indication function is rather stable for $z \in D$, we can choose a uniform cutoff value as

$$c = 0.35 \times \max_{z \in T} I_z.$$

The result is shown in Fig. 8.

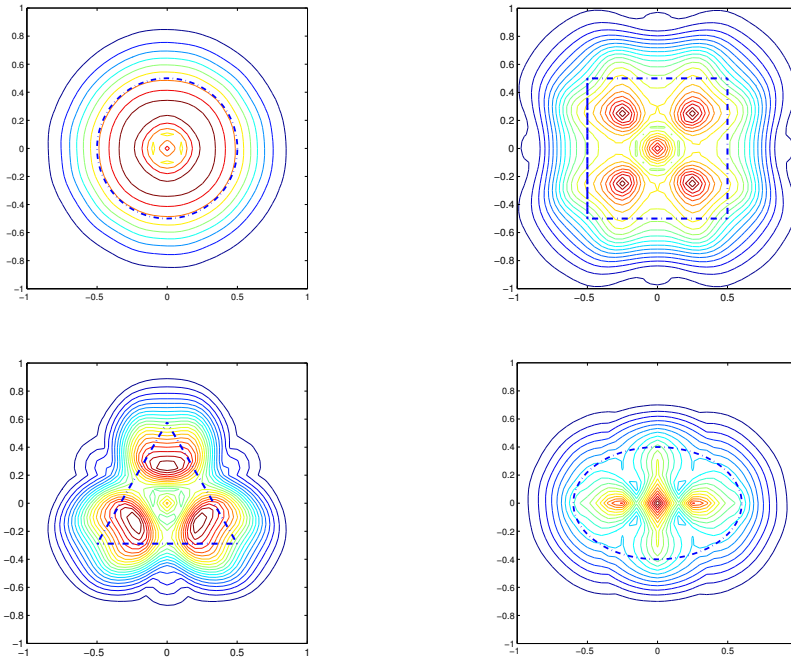


Figure 7: Reconstruction of the sound hard obstacles using the eigenvalue indicator on a larger interval.

4 Conclusions and future works

In this paper, we show that Neumann eigenvalues of sound hard obstacles can be estimated from the scattering data. Then we use the eigenvalue method to reconstruct the supports of sound hard obstacles. This work completes the results given in [7, 23, 24].

For z outside D but close to the boundary, numerical examples implies that some eigenvalues can still be reconstructed. This is an interesting phenomenon which requires further study. In our numerical simulations, we have collected the measurements on Γ for all the sources u^i on C . It is desirable to study limited aperture cases.

Acknowledgement

The research of XL was supported by the NNSF of China under grants 11101412 and 11071244. The research of JS was support in part by NSF under grant DMS-1016092 and the US Army Research Laboratory and the US Army Research Office under cooperative agreement number W911NF-11-2-0046.

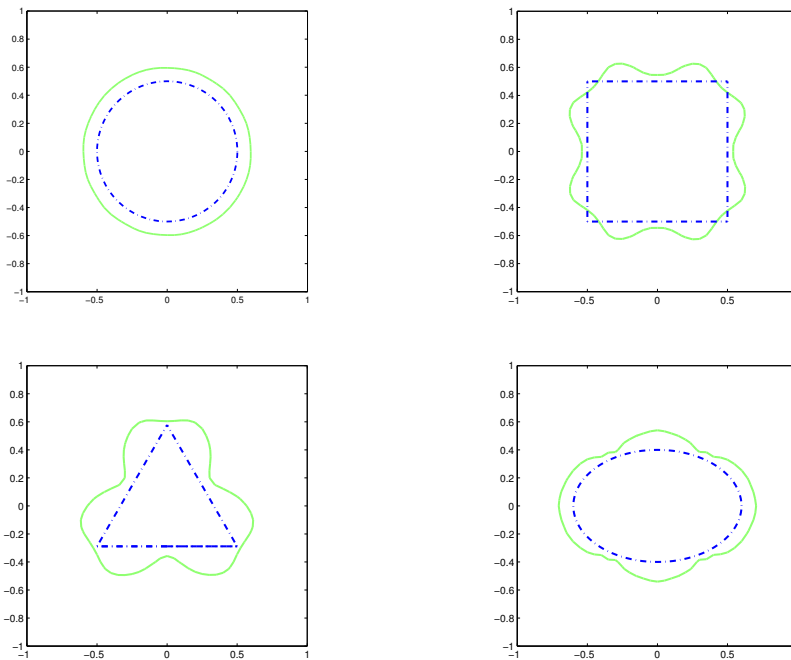


Figure 8: Single contour plots of the reconstructions.

References

- [1] R.A. Adams, Sobolev Spaces, Pure and Applied Mathematics, Vol. 65, Academic Press, New York, 1975.
- [2] H. F. Alqadah and N. Valdivia, *A frequency based constraint for a multi-frequency linear sampling method*, Inverse Problems 29 (2013), 095019.
- [3] T. Arens and A. Lechleiter, *The linear sampling method revisited*, J. Integral Equations Appl. 21 (2009), 179-202.
- [4] S.C. Brenner and L.R. Scott, The mathematical theory of finite elements methods, 2nd Edition, Texts in Applied Mathematics, Springer, New York, 2002.
- [5] I. Babuška and J. Osborn, Eigenvalue Problems, Handbook of Numerical Analysis, Vol. II, Finite Element Methods (Part 1), Edited by P.G. Ciarlet and J.L. Lions, Elsevier Science Publishers B.V. (North-Holland), 1991.
- [6] F. Cakoni and D. Colton, Qualitative methods in inverse scattering theory, Springer, Series on Interaction of Mathematics and Mechanics, 2006.
- [7] F. Cakoni, D. Colton and H. Haddar, *On the determination of Dirichlet and transmission eigenvalues from far field data*, C. R. Acad. Sci. Paris, Ser. I 348 (2010), 379-383.

- [8] F. Cakoni, D. Colton, P. Monk and J. Sun, *The inverse electromagnetic scattering problem for anisotropic media*, Inverse Problems 26 (2010), 074004.
- [9] Q. Chen, H. Haddar, A. Lechtleiter and P. Monk, *A sampling method for inverse scattering in the time domain*, Inverse Problems 26 (2010), 085001.
- [10] D. Colton, *Partial Differential Equations: An Introduction*, Dover, 1988.
- [11] D. Colton and H. Haddar, *An application of the reciprocity gap functional to inverse scattering theory*, Inverse Problems 21 (2005), 383–398.
- [12] D. Colton and R. Kress, *Inverse acoustic and electromagnetic scattering theory*, 2nd Edition, Springer Verlag (1998).
- [13] M. Di Cristo and J. Sun, *An inverse scattering problem for a partially coated buried obstacle*, Inverse Problems, Vol. 22, No. 6, 2006, 2331 – 2350.
- [14] R. Griesmaier, *Multi-frequency orthogonality sampling for inverse scattering problems*, Inverse Problems, Vol. 27 (2011), 085005.
- [15] B. Guzina, F. Cakoni and C. Bellis, *On the multi-frequency obstacle reconstruction via the linear sampling method*. Inverse Problems 26 (2010), no. 12, 125005.
- [16] M. Ikehata, *The enclosure method for inverse obstacle scattering problems with dynamical data over a finite time interval*, Inverse Problems 26(2010), 055010.
- [17] T. Kato, *Perturbation Theory of Linear Operators*, Springer-Verlag, Berlin, 1966.
- [18] A. Kirsch and N. Grinberg, *The factorization method for inverse problems*. Oxford Lecture Series in Mathematics and its Applications, 36. Oxford University Press, Oxford, 2008.
- [19] A. Kirsch and X. Liu, *A modification of the factorization method for the classical acoustic inverse scattering problems*, submitted, 2013.
- [20] R. Luke and R. Potthast, *The point source method for inverse scattering in the time domain*, Math. Methods Appl. Sci. 29(2006), 1501-1521.
- [21] P. Monk, *Finite Element Methods for Maxwell’s Equations*, Oxford University Press (2003).
- [22] P. Monk and J. Sun, *Inverse scattering using finite elements and gap reciprocity*, Inverse Problems and Imaging, Vol. 1, No. 4, 2007, 643–660.
- [23] J. Sun, *Estimation of transmission eigenvalues and the index of refraction from Cauchy data*, Inverse Problems 27 (2011), 015009.
- [24] J. Sun, *An eigenvalue method using multiple frequency data for inverse scattering problems*, Inverse Problems, 28(2012), 025012.